Stimulatory effect of hydrothermally synthesized biodegradable hydroxyapatite granules on osteogenesis and direct association with osteoclasts

Yoshinori Gonda[a, b], Koji Ioku[c], Yasuaki Shibata[a], Takatoshi Okuda[b], Giichiro Kawachi[d], Masanobu Kamitakahara[c], Hisashi Murayama[e], Katsumi Hideshima[f], Shimeru Kamihira[g], Ikuho Yonezawa[b], Hisashi Kurosawa[b], Tohru Ikeda[a, *]

[a]Department of Oral Pathology and Bone Metabolism, Unit of Basic Medical Sciences, Nagasaki University Graduate School of Biomedical Sciences, 1-7-1 Sakamoto, Nagasaki 852-8588, Japan

[b]Department of Orthopedic Surgery, School of Medicine, Juntendo University, 2-1-1 Hongo, Bunkyo-ku, Tokyo 113-8421, Japan

[c]Graduate School of Environmental Studies, Tohoku University, 6-6-20 Aramaki, Aoba-ku, Sendai, Miyagi 980-8579, Japan

[d]Department of Crystalline Materials Science, Graduate School of Engineering, Nagoya University, Furo-cyo, Chikusa-ku, Nagoya 464-8603, Japan

[e]Kureha Special Laboratory Co. Ltd., 3-26-2 Hyakunin-cho, Shinjuku-ku, Tokyo 169-8503, Japan

[f]Division of Laboratory Medicine, Nagasaki University Hospital of Medicine and Dentistry, 1-7-1 Sakamoto, Nagasaki 852-8501, Japan

[g]Department of Laboratory Medicine, Unit of Translational Medicine, Nagasaki University Graduate School of Biomedical Sciences, 1-12-4 Sakamoto, Nagasaki 852-8523, Japan

---

*Corresponding author. Tel./fax: +81 95 819 7644.

E-mail: tohrupth@nagasaki-u.ac.jp

Abstract

Calcium-deficient hydroxyapatite (HA) granules with a unique spherical shape were prepared using an applied hydrothermal method. Spherical stoichiometric HA granules were also prepared by normal sintering and both granules were used for implantation into rat tibiae to compare the biological responses to each implant. Twelve and 24 weeks after implantation, the volume of calcium-deficient HA granules was significantly less than that of stoichiometric HA granules, and the biodegradability of calcium-deficient HA granules was confirmed. The larger number of osteoclasts, larger osteoblast surface and larger bone volume in the implanted area of calcium-deficient HA than of stoichiometric HA suggested that osteoclastic resorption of calcium-deficient HA affected osteogenesis in that area. To analyze the direct contribution of osteoclasts to osteogenesis, C2C12 multipotent myoblastic cells, which have the potential to differentiate into osteoblasts in the presence of bone morphogenetic protein 2, were cultured with supernatants of osteoclasts cultured on calcium-deficient HA, stoichiometric HA, β-tricalcium phosphate disks or plastic dishes, or bone marrow macrophages cultured on plastic dishes. Supernatants of osteoclasts but not bone marrow macrophages stimulated the expression of Runx2 and osteocalcin in C2C12 cells in concert with bone morphogenetic protein 2. The expression of alkaline phosphatase was stimulated with supernatants of osteoclasts cultured on ceramic disks. These results suggested that osteoclasts produced certain soluble factors which stimulated osteoblastic differentiation and they were thought to be associated with the induction of a larger osteoblast surface and bone volume in the animals implanted with calcium-deficient HA granules.

Keywords: Hydroxyapatite; Bone graft; Cell culture; Osteoblast; Osteoclast

1. Introduction

Osteoconductivity is the ability to provide an appropriate scaffold or template for bone formation [1]. Hydroxyapatite (HA) is known to express potent osteoconductivity and has been used clinically as a bone substitute. HA is also known as a ceramic with an unbiodegradable nature when implanted into bone [2, 3], although a few reports have suggested that HA is resorbed in bone [4]. Beta-tricalcium phosphate (β-TCP) is another material frequently used as a bone substitute, and is expected to be replaced with bone tissue after implantation because of its biodegradable nature. When the bone defect is large, the provision of osteogenic cells has been shown to improve the replacement of β-TCP to bone tissue, and tissue engineering, which differentiates mesenchymal stem cells to osteoblasts on a ceramic scaffold, is thought to be an effective methods for bone regeneration [5-10].

Although osteoinduction by ceramics has been shown experimentally, the data vary, the mechanism remains uncertain and no bone substitute with osteoinductive potential has been used clinically so far [11, 12]; however, stimulatory effects for osteogenesis may be present in some kinds of ceramics [12-14]. Yokozeki et al. initially suggested that the microstructure of β-TCP affected osteogenesis in implanted bone [15].

We have developed HA and β-TCP, composed of unique rod-shaped particles, using the applied hydrothermal method [16, 17]. The mineral apposition rate (MAR) in the region implanted with hydrothermally synthesized β-TCP composed of rod-shaped particles was significantly higher than β-TCP prepared by normal sintering [18]. Additionally, we have shown that the structure of particles composed of β-TCP affected not only osteogenesis in the implanted region but also the metabolism of newly formed bone, which was formed in place of β-TCP. Recently, we implanted hydrothermally synthesized HA, composed of rod-shaped particles (HHA), to rabbit femurs as a bone substitute and showed that MAR in the region implanted with HHA was significantly higher than stoichiometric HA composed of globular-shaped particles, which were prepared by normal sintering (SHA) [19]. These data strongly suggested that the microstructures of ceramics affected the biological activity of osteoblasts. In these experiments, HHA was biodegradable in implanted bone tissue, and higher MAR in specimens implanted with HHA might be associated with osteoclastic

resorption of HHA. Biphagic calcium phosphate and octacalcium phosphate have also been shown to be resorbed by osteoclasts [20, 21]. In addition, it was shown that the amount of newly formed bone in the region implanted with biphagic calcium phosphate or octacalcium phosphate is more than that of HA using animal models [12, 22]. These data also supported that osteoclastic resorption of bone substitutes affected osteogenesis in the implanted region.

Considering the clinical application of bone substitutes, a block-shaped bone substitute is thought to be useful for fixing of fractures and filling defects in heavily weighted regions of the bone. On the other hand, granular bone substitutes should be useful for filling defects in unweighted or lightly-weighted regions of the bone. Granular bone substitutes are easily applicable in many kinds of bone defects, and are expected to combine with the bone quickly, because there are many spaces which profit from the invasion of endothelial and osteoblastic cells around the granules; hence, the development of a granular bone substitute with a functional shape is also very important for clinical applications.

Previously, we established a method to prepare unique spherical granules of HHA, SHA and β-TCP [23, 24]. In this study, we used originally developed spherical HHA and SHA granules as bone substitutes to fill bone defects created in rat tibiae; only HHA granules were biodegradable. HHA granules had more osteoclasts on the surface than SHA and induced more bone tissue than spherical SHA granules in the implanted region. The biological mechanism to increase osteogenesis by biodegradable ceramics remained uncertain; hence, this was studied by in vitro assay systems using osteoclasts and C2C12 multipotent myoblastic cells. By culturing C2C12 cells with supernatants of osteoclasts cultured on ceramics, the association of osteoclasts with osteoblastic differentiation was analyzed.

2. Materials and methods

2.1. Preparation of ceramics

Alpha-TCP powder (Taihei Chemical Ind. Co. Ltd., Saitama, Japan) was mixed and kneaded with 10% gelatine solution, and dropped into a stirred oil bath heated at 80 ^{o}C. The bath was then chilled on ice and spherical α-TCP/gelatine granules formed. The granules were separated from the oil, rinsed and sintered at 1200 ^{o}C for 10 min to remove gelatine and to maintain the crystal phase of α-TCP. The formed α-TCP granules were set in a 105 cm^3 autoclave at 160 ^{o}C under saturated water vapour pressure for 20 h. Synthesized HHA granules were sieved and granules 0.5 to 0.6 mm diameter were used for experiments. Spherical SHA granules were prepared by sintering at 900 ^{o}C for 3 h from the same chemical purity grade HA powders with stoichiometric composition. The porosity of HHA and SHA granules was designed to be 70%. Rod-shaped particles of spherical HHA granules (Fig. 1a, c) and globular-shaped particles of spherical SHA granules (Fig. 1 b, d) were confirmed using a scanning electron microscope. Synthesized HHA and SHA granules were analyzed by powder X-ray diffractometry with graphite-monochromatized CuKα radiation, operating at 40 kV and 20 mA (XRD; Multi Flex, Rigaku, Tokyo, Japan). No phase other than HA was detected for HHA and SHA (Fig. 1e, f). When HHA was sintered at 1200 ^{o}C, decomposition of HA to β-TCP was detected because the HHA granules were nonstoichiometric HA of calcium-deficient composition. There was no decomposition as a result of sintering in the case of SHA granules because SHA was stoichiometric (data not shown). These results corresponded to chemical analysis by ICP-MS (SPQ9000; Seiko Inst., Tokyo, Japan).

Disks for in vitro analyses were made by the sintering technique. The slurry of β-TCP with polyvinyl alcohol was prepared at room temperature. To remove bubbles, the slurry was kept under a vacuum. The slurry was formed into a 25 mm diameter disk shape by uniaxial compressing. The formed disks with polyvinyl alcohol were dried and sintered at 900 ºC for 3 h to prepare β-TCP disks. Some of the samples were set in an autoclave at 160 ^{o}C under saturated water vapour pressure for 21 h to prepare HHA disks. SHA disks were prepared from stoichiometric HA powder (Ube Material Industries Ltd., Yamaguchi, Japan) by normal sintering at 900 ^{o}C for 3 h in air. Synthesized β-TCP, HHA and SHA

disks were also analyzed by powder X-ray diffractometry as described above, and the purity and uniformity of these materials were confirmed (data not shown).

2.2. Animals and operative procedures

Forty-eight female 8-week-old Wistar rats were anesthetized with an intraperitoneal injection of ketamine (40 mg/kg body weight) and xylazine (3 mg/kg body weight) before surgery. Under sterile conditions, the proximal metaphysis and medial collateral ligament of the knee were exposed. A dead-end bone defect 2 mm in diameter and 3 mm in depth was created in the medial cortex of the tibia just distal to the epiphyseal growth plate using a Kirschner's wire. The orientation of the defect was perpendicular to the sagittal axis of the tibia (Fig. 2a, b). The defect was irrigated with saline, 30 mg HHA or SHA granules were implanted into the defect, and the wound was sutured layer by layer (Fig. 2c). Four, 8, 12 and 24 weeks after the operation, animals were euthanized, operated bones were resected and undecalcified bone tissue sections were made from the resected bones. Animals rearing and experiments were performed at the Biomedical Research Center, Center for Frontier Life Sciences, Nagasaki University, following the Guidelines for Animal Experimentation of Nagasaki University (Approval No. 0703010564, 0704190571).

2.3. Histological analyses

All harvested tissue specimens were fixed in 4% formaldehyde in 0.1 M phosphate buffer (pH 7.2), embedded in 2-hydroxyethyl methacrylate/methyl methacrylate/2-hydroxyethyl acrylate mixed resin, and sectioned 3 μm thick. These sections were stained by the method of Giemsa or histochemically stained for tartrate-resistant acid phosphatase (TRAP) activity or alkaline phosphatase (ALP) activity. TRAP activity was stained as described previously [25]. Staining for ALP activity was performed using 0.2 M Tris-HCl buffer (pH. 8.5) as a reaction buffer. In this study, fast red RC salt (F5146; Sigma, St. Louis, MO) and fast blue BB salt (F3378; Sigma) were used as couplers to detect TRAP and ALP activities, respectively. Sections stained for TRAP activity and ALP activity were counterstained with hematoxylin and nuclear fast red,

respectively.

Histomorphometric analyses were performed using the Osteoplan II system (Carl Zeiss, Thornwood, NY). In addition to parameters used under standardized nomenclature [26], original parameters were also used to calculate bone substitutes. Bone volume + implant volume/tissue volume (BV+Imp.V/TV, %), implant volume/tissue volume (Imp.V/TV), net bone volume/tissue volume (BV/TV), osteoblast surface/bone surface (Ob.S/BS, %) and the number of osteoclasts/bone perimeter (N.Oc/B.Pm, per 100 mm) were calculated for each sample in a 0.6 mm x 1.8 mm square, which was aligned on the medial longitudinal axis of the tibia and arranged centrally in a created bone defect. The change in implant volume per tissue volume was evaluated using a parameter Imp.V/TV, and displacement of the implant to newly formed bone was evaluated using a parameter BV/TV. Osteoclasts were defined as multinucleated cells in contact with the bone or bone substitutes. To calculate the parameters described above, sections stained with Giemsa's method were used. Data are expressed as the mean ± s.d. Statistical differences were evaluated with the t-test and P value < 0.05 was considered significant.

2.4. In vitro experiments

In vitro osteoclastogenesis was performed as follows. Mouse bone marrow macrophages prepared from the femora and tibiae of 5-week-old female ddY mice were expanded in vitro in α-minimum essential medium supplemented with 10% fetal bovine serum and 30 ng/ml macrophage colony-stimulating factor (Sigma). The macrophages (1 x 10^4 cells/cm^2) were mixed with NIH3T3 cells expressing human RANKL cDNA (1 x 10^4 cells/cm^2) [25], and seeded in 6-well plates into which one β-TCP, SHA or HHA disk of 25 mm diameter was inserted. All ceramic disks were presoaked in α-minimum essential medium supplemented with 10% fetal bovine serum for 3 weeks before being used for experiments. The soaking medium was changed twice a week. The medium of the cultures was changed every other day up to day 18 of the culture period. Culture supernatants of numerous osteoclasts at 8, 10 and 12 days of culture were collected, stored at 4 ºC and used for the following experiments. In addition, a culture supernatant of osteoclasts cultured as described in plates without a ceramic disc and a culture supernatant

of mouse bone marrow macrophages were also used for experiments.

C2C12 myoblastic cells, which possess the potential to differentiate into osteoblasts when stimulated with bone morphogenetic protein 2 (BMP-2) [27], were cultured in 60% Dulbecco's minimum essential medium including 2.5% fetal bovine serum and 40% of each culture supernatant supplemented with 200 ng/ml BMP-2 (R&D Systems, CA). As a control, α-minimum essential medium supplemented with 10% fetal bovine serum was used in place of the culture supernatant. The calcium concentration in each mixed culture medium was analyzed using a JCA-BM12 automatic analyzer (JEOL, Tokyo, Japan) and Diacolor Liquid Ca Kit (Toyobo, Osaka, Japan) following routine biochemical examination in Nagasaki University Hospital.

Real-time PCR was performed using cDNA synthesized from total RNA extracted from C2C12 cells described above with Premix EX-Taq (TAKARA, Shiga, Japan) and a Mx 3005P QPCR System (Stratagene, CA) following the manufacturer's instructions. Primers used for the PCR reaction were as follows: Runx2: Mm00501580_m1, Alkaline phosphatase (ALP): Mm00475834_m1, Osteocalcin: Mm03413826_mH, Gapdh: Mm99999915_g1 (all from Applied Biosystems, CA). Values for each gene were normalized to the relative quantity of glyceraldehyde-3-phosphate dehydrogenase mRNA in each sample. Data were evaluated using the t-test with data from 4 identical experiments and P value < 0.05 was considered significant.

3. Results

3.1. Histological analyses

Light microscopic views of specimens stained with Giemsa's method are shown in Fig. 3. Implanted materials appeared dark and were distinguishable from bright bone tissue and blue-stained bone marrow tissue including scattered whitish adipose tissue and dark blue-stained fibrous tissues (arrows). In specimens implanted with HHA (Fig. 3a−d) and SHA (Fig. 3e−h), a large amount of implants could be recognized and mosaic hard tissue composed of implanted granules and bone tissue was formed. It was clear that a large amount of bone tissue formed around implants from 4 weeks after the operation in specimens implanted with HHA and SHA. The total amount of the hard tissue including implants and newly formed bone, was much larger than the surrounding trabecular bones (Fig. 3). Additionally, in specimens 4, 8 and 12 weeks after implantation of HHA, connective tissue composed of fibroblastic cells was seen (Fig. 3a−c, arrows). This was also observed around SHA granules in some specimens, although no photograph is shown. After combining with the bone, both HHA and SHA granules tended to be broken down into smaller round pieces and this tendency become greater in later stages after the operation (Fig. 3c, d, g, h).

Interestingly, in some portions of residual HHA and SHA granules 12 and 24 weeks after the operation, composites of ceramic particles and bone tissue were formed (Fig. 4a). Arrowheads indicate the border between an implanted HHA granule and surrounding bone tissue. Figure 4b shows the histological findings of an implanted HHA granule without bone inclusion. Numerous fine rod-shaped particles were seen.

3.2. Histochemical analyses

The activities of one of the biochemical markers for osteoclasts, TRAP, and one of the biochemical markers for osteoblasts, ALP, were analyzed histochemically. Many TRAP-positive multinucleated cells were observed on the surface of implants and bone tissue throughout the experimental period in specimens implanted with HHA and SHA (Figs. 5 and 6, a−d). On the surface of HHA, relatively large decay (Fig. 5a, arrows) and resorption lacunae-like structures (Fig. 5b−d, arrows) were frequently seen. This surface

decay was more obvious in HHA than in SHA, but surface irregularity of the implants was also seen in SHA to some extent and was sometimes difficult to distinguish from resorption lacunae (Fig. 6a, b, arrows). ALP-positive cells were detected on the surface of bone tissue (Fig. 5g, h, Fig. 6e−h, arrowheads). ALP-positive cells were also observed in the bone marrow area (Fig. 5f, arrows). The fibroblastic cells shown in Fig. 3a−c (arrows) were ALP-positive, and ALP activity in Fig. 5f is a higher magnification view of some of these cells. Once residual implants were combined with newly formed bone, osteoclasts and osteoblasts were found in only small bone marrow spaces, including small blood vessels (Figs. 5d, h, 6c, d, g, h).

3.3. Histomorphometry

BV+Imp.V/TV was maintained almost equally and was not significantly different between specimens implanted with HHA and SHA throughout the experimental period (Fig. 7a). The net implant volume was evaluated by Imp.V/TV, tended to gradually decrease in specimens implanted with HHA, and was significantly lower than specimens implanted with SHA 12 and 24 weeks after the operation (Fig. 7b). To evaluate the displacement of the implant to newly formed bone, BV/TV was calculated, tended to gradually increase in specimens implanted with HHA, and was significantly higher than specimens implanted with SHA 12 and 24 weeks after the operation (Fig. 7c). The composite composed of bone and HHA or SHA (Fig. 4a) was included in “Imp.V” when histomorphometric analyses were performed. Both Ob.S/BS and N.Oc/B.Pm tended to be higher in specimens implanted with HHA than in specimens implanted with SHA throughout the experimental period. Ob.S/BS and N.Oc/B.Pm in specimens implanted with HHA were significantly higher than SHA 12 and 24 weeks after the operation and 4, 8 and 24 weeks after the operation, respectively (Fig. 7d, e).

3.4. In vitro analyses

C2C12 myoblastic cells, which differentiate into osteoblastic cells in the presence of BMP-2, were cultured using supernatants of osteoclasts cultured on β-TCP, SHA, HHA or plastic dishes, or using a supernatant of bone marrow macrophages cultured on plastic

dishes. Except for a culture medium including 40% of the supernatant of osteoclasts cultured on SHA, the calcium concentration in each medium ranged from 7.56 to 7.78 mg/dl, which was similar to that in control medium, including 40% of fresh α-minimum essential medium supplemented with 10% fetal bovine serum. Only the calcium concentration of the medium, including 40% of culture supernatant of osteoclasts cultured on SHA, was lower than the others (Fig. 8a). These supernatants did not affect the expression of Runx2, osteocalcin or ALP in C2C12 cells in the absence of BMP-2 (data not shown). The stimulatory effect of these culture supernatants on these expressions in C2C12 cells was then assessed in the presence of a low level (200 ng/ml) of BMP-2. As shown in Fig. 8b, the expression of Runx2 was significantly increased in C2C12 cells cultured with media including any kind of supernatants of osteoclasts compared to C2C12 cells cultured with medium including the supernatant of bone marrow macrophages or control medium including fresh α-minimum essential medium in place of the culture supernatant. The expression of Runx2 in C2C12 cells cultured with the supernatant of bone marrow macrophages was almost the same level as the control, and no significant difference was detected in the expression of Runx2 in C2C12 cells cultured with any supernatant of osteoclasts (Fig. 8b).

Osteocalcin was highly expressed in C2C12 cells cultured with supernatants of osteoclasts cultured on ceramic disks. Statistical analyses indicated that the expression of osteocalcin was significantly higher in C2C12 cells cultured with any supernatant than the control. The expression of osteocalcin in C2C12 cells cultured with the supernatant of osteoclasts on plastic dishes was significantly higher than the supernatant of bone marrow macrophages, and the expression of osteocalcin in C2C12 cells cultured with the supernatant of osteoclasts on β-TCP or SHA disks was significantly higher than the expression in C2C12 cells cultured with the supernatant of osteoclasts on plastic dishes (Fig. 8c). The expression of osteocalcin in C2C12 cells cultured with the supernatant of HHA tended to be higher than the expression in C2C12 cells cultured with the supernatant of osteoclasts on plastic dishes, although it was not significant (Fig. 8c). The expression of osteocalcin in C2C12 cells cultured with the supernatant of macrophages was significantly higher than that of the control (Fig. 8c).

ALP was highly expressed only in C2C12 cells cultured with supernatants of osteoclasts cultured on ceramic disks. In these cells, the expression of ALP was significantly higher than that in C2C12 cells cultured with the supernatant of osteoclasts on plastic dishes, with the supernatant of bone marrow macrophages, and cultured with control medium. The expression of ALP in C2C12 cells cultured with the supernatant of osteoclasts on plastic dishes and cultured with a supernatant of bone marrow macrophages was not significantly different from that cultured with control medium (Fig. 8d).

Discussion

We have already reported that cylindrical HHA blocks 6 mm in diameter and 10 mm in length slowly biodegraded in the rabbit femur [19]. In the present study, we confirmed that spherical HHA granules also slowly biodegraded in the rat tibia. Granules have advantages in that they are widely applicable to various bone defects, and have much more surface area than a block when filled in an equivalent bone defect, and intergranular space is thought to benefit bone tissue invasion. Additionally, our uniform-sized spherical granules were thought to have advantages to achieve stable and better prognosis than irregular-shaped granules, as suggested previously [24].

Although the biodegradability of HHA granules was slow (Fig. 7b), HHA blocks implanted in rabbit femurs were mostly resorbed 72 weeks after implantation and replaced with bone tissue. This finding was strikingly different from SHA implants, which almost completely remained [19]. Considering these previous findings in rabbit experiments, the remaining HHA granules, which formed mosaic tissue composed of HHA and bone tissue up to 24 weeks after the operation, were thought to express modest biodegradability and were expected to be replaced with bone tissue over a longer period. Additionally, mosaic tissue composed of bone and HHA or SHA granules was thought to have higher mechanical strength than the ceramic itself, and slow biodegradability of HHA may not be a serious problem when applied for clinical treatment, although precise studies to analyze the mechanical strength of mosaic tissue are needed. Using a rabbit implantation model, we showed that the implantation of a bone substitute with excess biodegradability corrupted normal bone metabolism and caused the resorption of regenerated bone formed in place of the bone substitute [18]. Hence, the slow biodegradability of HHA granules might not be a disadvantage for clinical application.

In this study, we found a composite composed of ceramic with bone inclusion (Fig. 5a). One of the mechanisms of composite formation was thought to be the invasion of bone tissue from macropores of the ceramic. Another possibility was suspected to be increased local calcium concentration by degradation of the ceramic. Although the composite, which was seen in both HHA and SHA, was formed irrespective of the biodegradability of the ceramic, the calcium concentration of the supernatant of osteoclasts cultured on SHA

was lower than the others (Fig. 8a), and SHA was thought to have the ability to adsorb calcium. This calcium adsorption might contribute to composite formation in SHA. Analyses of the physical nature of the composite and in vitro study using body fluids are also needed.

Bone metabolism is strictly regulated. Under physiological conditions, the amount of bone formation and bone resorption are regulated to be equal. Hence, it has been hypothesized that osteogenesis and osteolysis influence each other to maintain the homeostasis of bone metabolism. The expression of one of the most important factors for osteoclastogenesis, RANKL by osteoblasts induces osteoclastogenesis and reveals the regulation of osteolysis by osteogenic cells [28]. It has been suggested that certain proteins included in bone were released by osteoclastic bone resorption and contributed to osteogenesis [18, 19, 22]. Osteoclasts might also directly contribute to osteogenesis through increased local calcium concentration and still unknown functions. Interestingly, osteoclasts were recognized not only on HHA but also on SHA for a relatively long period, but N.Oc/B.Pm in the implanted area of HHA was significantly higher than that of the implanted area of SHA. In addition to the biodegradability of HHA granules, we detected significantly more bone formation in the region implanted with HHA granules compared to the region implanted with SHA granules (Fig. 7a). These data also raised the possibility of osteoclastic stimulation of osteogenesis.

We tried to clarify whether osteoclasts affected the differentiation of osteoblasts using an in vitro assay system of osteoclastogenesis and osteoblastic differentiation. In this study, we showed for the first time that certain soluble factor(s) in culture supernatants of osteoclasts stimulated the differentiation of osteoblasts (Fig. 8). Although culture supernatants of osteoclasts did not solely differentiate osteoblasts, they stimulated the expression of Runx2 and osteocalcin in C2C12 cells in concert with BMP-2. These data showed that the soluble factor(s) in culture supernatants was other than BMP-2. It was of interest that the stimulatory effects of supernatants of osteoclasts were influenced by the culture condition. The Runx2 binding domain is present in the promoter region of the osteocalcin gene and the expression of Runx2 directly affects the expression of osteocalcin. In this study, supernatants of any osteoclasts evenly stimulated the expression of Runx2,

but supernatants of osteoclasts cultured on ceramic disks stimulated the differentiation of C2C12 cells more potently than that of a supernatant of osteoclasts cultured on plastic dishes. These data suggest that osteoclasts cultured on ceramic disks preferentially express factors other than Runx2 which stimulate the differentiation and maturation of osteoblasts. The influence of supernatants of osteoclasts on ALP expression was more striking. The expression of ALP was significantly higher only in C2C12 cells cultured with supernatants of osteoclasts cultured on ceramic disks (Fig. 8c). The biological difference between osteoclasts cultured on ceramic disks and on plastic dishes has not been characterized precisely. Osteoclasts cultured on ceramic disks were thought to actually resolve β-TCP and HHA, and to try to resolve SHA. Hence, it was highly possible that osteoclasts on these ceramics were more biologically active than osteoclasts on plastic disks in the activity of proton ATPase, calcium channels, calcium pumps and so on, and certain soluble factors which stimulate the expression of ALP might be synthesized only in active osteoclasts.

We have suggested that the structure of rod-shaped particles of our ceramics also affected osteogenesis, although the precise biological mechanism remains uncertain [18, 19]. Additionally, rod-shaped particles composed of HHA have polarity with a prolonged c-axis, and the surface was thought to have many positive-charged sites. The preferential adsorptive nature of HHA for acidic protein [29] also supports this hypothesis. The surface charge of ceramics was suggested to stimulate osteogenesis [30, 31], and not only adsorbed acidic proteins in HHA, but also the surface charge of HHA may stimulate osteogenesis.

4. Conclusion

We have established a unique method to make spherical granules of calcium-deficient HA composed of rod-shaped particles (HHA) using an applied hydrothermal method. HHA granules biodegraded by osteoclastic resorption in contrast to spherical granules of stoichiometric HA (SHA). Histomorphometric analyses showed that the number of osteoclasts and the amount of newly formed bone were significantly increased in the specimens implanted with HHA compared to SHA. In vitro studies showed that the supernatants of osteoclasts stimulated the expression of Runx2 and osteocalcin, and supernatants of osteoclasts cultured on HHA, SHA and β-TCP disks, but not plastic dishes, stimulated the expression of ALP in C2C12 multipotent myoblastic cells in the presence of BMP-2. In vitro studies suggested that osteoclasts produced certain soluble factor(s) which stimulate osteoblastic differentiation, and osteoclasts cultured on HHA, SHA and β-TCP synthesized distinct soluble factor(s) which stimulate the expression of ALP in C2C12 cells. A composite composed of ceramic with bone inclusion was shown to be formed in both implanted HHA and SHA granules. The composite was thought to be formed by the invasion of bone tissue into macropores of porous ceramics, but increased local calcium concentration by HHA degradation and the calcium adsorptive nature of SHA might also contribute to composite formation.

Acknowledgments

This work was supported by a Grant-in-Aid from the Ministry of Education, Culture, Sports, Science and Technology of Japan (Grant nos. 18390519 and 18659541) and “Ground-based Research Program for Space Utilization” promoted by the Japan Space Forum.

References

1. LeGeros RZ. Properties of osteoconductive biomaterials: calcium phosphates. Clin Orthop Relat Res 2002;395:81-98.

2. Hoogendoorn HA, Renooij W, Akkermans LM, Visser W, Wittebol P. Long-term study of large ceramic implants (porous hydroxyapatite) in dog femora. Clin Orthop Relat Res 1984;187:281-288.

3. Bucholz RW, Carlton A, Holmes R. Interporous hydroxyapatite as a bone graft substitute in tibial plateau fractures. Clin Orthop Relat Res 1989;240:53-62.

4. Goto T, Kojima T, Iijima T, Yokokura S, Kawano H, Yamamoto A, et al. Resorption of synthetic porous hydroxyapatite and replacement by newly formed bone. J Orthop Sci 2001;6:444-447.

5. Bruder SP, Kraus KH, Goldberg VM, Kadiyala S. The effect of implants loaded with autologous mesenchymal stem cells on the healing of canine segmental bone defects. J Bone Joint Surg Am 1998;80:985-996.

6. Kon E, Muraglia A, Corsi A, Bianco P, Marcacci M, Martin I, et al. Autologous bone marrow stromal cells loaded onto porous hydroxyapatite ceramic accelerate bone repair in critical-size defects of sheep long bones. J Biomed Mater Res 2000;49:328-337.

7. Lieberman JR, Daluiski A, Einhorn TA. The role of growth factors in the repair of bone. Biology and clinical applications. J Bone Joint Surg Am 2002;84-A:1032-1044.

8. Kasten P, Luginbuhl R, van Griensven M, Barkhausen T, Krettek C, Bohner M, et al. Comparison of human bone marrow stromal cells seeded on calcium-deficient hydroxyapatite, beta-tricalcium phosphate and demineralized bone matrix. Biomaterials 2003;24:2593-2603.

9. Uemura T, Dong J, Wang Y, Kojima H, Saito T, Iejima D, et al. Transplantation of cultured bone cells using combinations of scaffolds and culture techniques. Biomaterials 2003;24:2277-2286.

10. Wang J, Asou Y, Sekiya I, Sotome S, Orii H, Shinomiya K. Enhancement of tissue engineered bone formation by a low pressure system improving cell seeding and medium perfusion into a porous scaffold. Biomaterials 2006;27:2738-2746.

11. Kasten P, Vogel J, Luginbuhl R, Niemeyer P, Tonak M, Lorenz H, et al. Ectopic

bone formation associated with mesenchymal stem cells in a resorbable calcium deficient hydroxyapatite carrier. Biomaterials 2005;26:5879-5889.

12. Habibovic P, Sees TM, van den Doel MA, van Blitterswijk CA, de Groot K. Osteoinduction by biomaterials-physicochemical and structural influences. J Biomed Mater Res A 2006;77:747-762.

13. Li X, van Blitterswijk CA, Feng Q, Cui F, Watari F. The effect of calcium phosphate microstructure on bone-related cells in vitro. Biomaterials 2008;29:3306-3316.

14. Fellah BH, Gauthier O, Weiss P, Chappard D, Layrolle P. Osteogenicity of biphasic calcium phosphate ceramics and bone autograft in a goat model. Biomaterials 2008;29:1177-1188.

15. Yokozeki H, Hayashi T, Nakagawa T, Kurosawa H, Shibuya K, Ioku K. Influence of surface microstructure on the reaction of the active ceramics in vivo. J Mater Sci Mater Med 1998;9:381-384.

16. Ioku K, Minagi H, Yonezawa I, Okuda T, Kurosawa H, Ikeda T, et al. Porous ceramics of β-tricalcium phosphate composed of rod-shaped particles. Arch Bioceram Res 2004;4:121-124.

17. Ioku K, Kawachi G, Yamasaki M, Toda H, Fujimori H, Goto S. Hydrothermal preparation of porous hydroxyapatite with tailrod crystal surface Key Eng Mater 2005;288-289:521-524.

18. Okuda T, Ioku K, Yonezawa I, Minagi H, Kawachi G, Gonda Y, et al. The effect of the microstructure of beta-tricalcium phosphate on the metabolism of subsequently formed bone tissue. Biomaterials 2007;28:2612-2621.

19. Okuda T, Ioku K, Yonezawa I, Minagi H, Gonda Y, Kawachi G, et al. The slow resorption with replacement by bone of a hydrothermally synthesized pure calcium-deficient hydroxyapatite. Biomaterials 2008;29:2719-2728.

20. Daculsi G. Biphasic calcium phosphate concept applied to artificial bone, implant coating and injectable bone substitute. Biomaterials 1998;19:1473-1478.

21. Imaizumi H, Sakurai M, Kashimoto O, Kikawa T, Suzuki O. Comparative study on osteoconductivity by synthetic octacalcium phosphate and sintered hydroxyapatite in rabbit bone marrow. Calcif Tissue Int 2006;78:45-54.

22. Suzuki O, Kamakura S, Katagiri T, Nakamura M, Zhao B, Honda Y, et al. Bone formation enhanced by implanted octacalcium phosphate involving conversion into Ca-deficient hydroxyapatite. Biomaterials 2006;27:2671-2681.

23. Takahashi T, Kamitakahara M, Kawachi G, Ioku K. Preparation of spherical porous granules composed of rod-shaped hydrixyapatite and evaluation of their protein adsorption properties. Key Eng Mater 2008;361-363:83-86.

24. Gonda Y, Ioku K, Okuda T, Kawachi G, Yonezawa I, Kurosawa H, et al. Application of newly developed globular-shaped granules of beta-tricalcium phosphate for bone substitutes. Key Eng Mater 2008;361-363:1013-1016.

25. Ikeda T, Kasai M, Suzuki J, Kuroyama H, Seki S, Utsuyama M, et al. Multimerization of the receptor activator of nuclear factor-kappaB ligand (RANKL) isoforms and regulation of osteoclastogenesis. J Biol Chem 2003;278:47217-47222.

26. Parfitt AM, Drezner MK, Glorieux FH, Kanis JA, Malluche H, Meunier PJ, et al. Bone histomorphometry: standardization of nomenclature, symbols, and units. Report of the ASBMR Histomorphometry Nomenclature Committee. J Bone Miner Res 1987;2:595-610.

27. Zhao B, Katagiri T, Toyoda H, Takada T, Yanai T, Fukuda T, et al. Heparin potentiates the in vivo ectopic bone formation induced by bone morphogenetic protein-2. J Biol Chem 2006;281:23246-23253.

28. Suda T, Takahashi N, Udagawa N, Jimi E, Gillespie MT, Martin TJ. Modulation of osteoclast differentiation and function by the new members of the tumor necrosis factor receptor and ligand families. Endocr Rev 1999;20:345-357.

29. Kawachi G, Sasaki S, Nakahara K, Ishida EH, Ioku K. Porous apatite carrier prepared by hydrothermal method. Key Eng Mater 2006;309-311:935-938.

30. Ohgaki M, Kizuki T, Katsura M, Yamashita K. Manipulation of selective cell adhesion and growth by surface charges of electrically polarized hydroxyapatite. J Biomed Mater Res 2001;57:366-373.

31. Itoh S, Nakamura S, Kobayashi T, Shinomiya K, Yamashita K. Effect of electrical polarization of hydroxyapatite ceramics on new bone formation. Calcif Tissue Int 2006;78:133-142.

Figure legends

Fig. 1. Scanning electron micrographs of the overview (a, b) and the microstructure (c, d) of HHA (a, c) and SHA (b, d) granules. (e, f) X-ray diffractometry (XRD) of implants used in this study. XRD patterns of HHA (e) and SHA (f) granules.

Fig. 2. Schematic drawings of anterior-posterior view (a) and lateral view (b) of the operated proximal tibia. (c) Photographic view of the created bone defect and implanted granules.

Fig. 3. Histological appearance of undecalcified sections of rat tibiae implanted with HHA (a−d) and SHA (e−h). Sections were stained by Giemsa's method. Arrows indicate fibrous connective tissue formed around implants.

Fig. 4. High-power magnification views of composite formed in an implanted HHA granule (a) and a residual HHA granule implanted into bone (b). Arrowheads represent the border between an implanted granule and surrounding bone tissue. Asterisks (*) represent bone tissue. Sections were stained with hematoxylin and viewed using polarization filters.

Fig. 5. Histochemical appearance of undecalcified sections of rat tibiae implanted with HHA stained for TRAP activity (a−d) and for ALP activity (e−h). Arrows in a−d indicate the surface of resorption lacunae-like decay found on HHA granules. Arrows in f indicate ALP-positive cells in the bone marrow area and arrowheads in g and h indicate ALP-positive osteoblasts on the surface of bone tissue or implants.

Fig. 6. Histochemical appearance of undecalcified sections of rat tibiae implanted with SHA stained for TRAP activity (a−d) and for ALP activity (e−h). Arrows in a−d indicate decay found on the surface of SHA granules. Arrowheads indicate ALP-positive osteoblasts on the surface of bone tissue.

Fig. 7. Histomorphometry of implants and bone tissue in specimens 4, 8, 12 and 24 weeks after the operation. Parameters of the amount of implants and bone tissue for the amount of total tissue, BV+Imp.V/TV (a), the net amount of implants for the amount of total tissue, Imp.V/TV (b) and the net amount of newly formed bone for the amount of total tissue, BV / TV (c) were compared between specimens implanted with HHA (dark gray columns) and specimens implanted with SHA (light gray columns). Parameters for osteoblasts, Ob.S/B.S (d) and for osteoclasts, N.Oc/B.Pm (e) were also compared. Six samples for each experiment were analyzed for the acquired data. (*$P < 0.05$, **$P < 0.01$)

Fig. 8. In vitro differentiation of C2C12 cells with culture supernatants of osteoclasts. (a) Calcium concentration of media using this assay. Beta-TCP, SHA and HHA represent medium including 40% of osteoclast supernatant cultured on β-TCP disks, HHA disks and SHA disks, respectively. Plastic represents medium including 40% of osteoclast supernatant cultured on dishes without ceramic disks. Mph represents medium including 40% of bone marrow macrophage supernatant, and Control represents medium including 40% of fresh culture medium for osteoclasts. (b−d) Real-time PCR analyses for the expression of osteoblast markers. Relative quantity of Runx2 (b), osteocalcin (c) and ALP (d) mRNA expression. The β-TCP, SHA, HHA, Plastic, Mph and Control represent C2C12 cells cultured with each supernatant described above, respectively. (*$P < 0.05$, **$P < 0.01$)

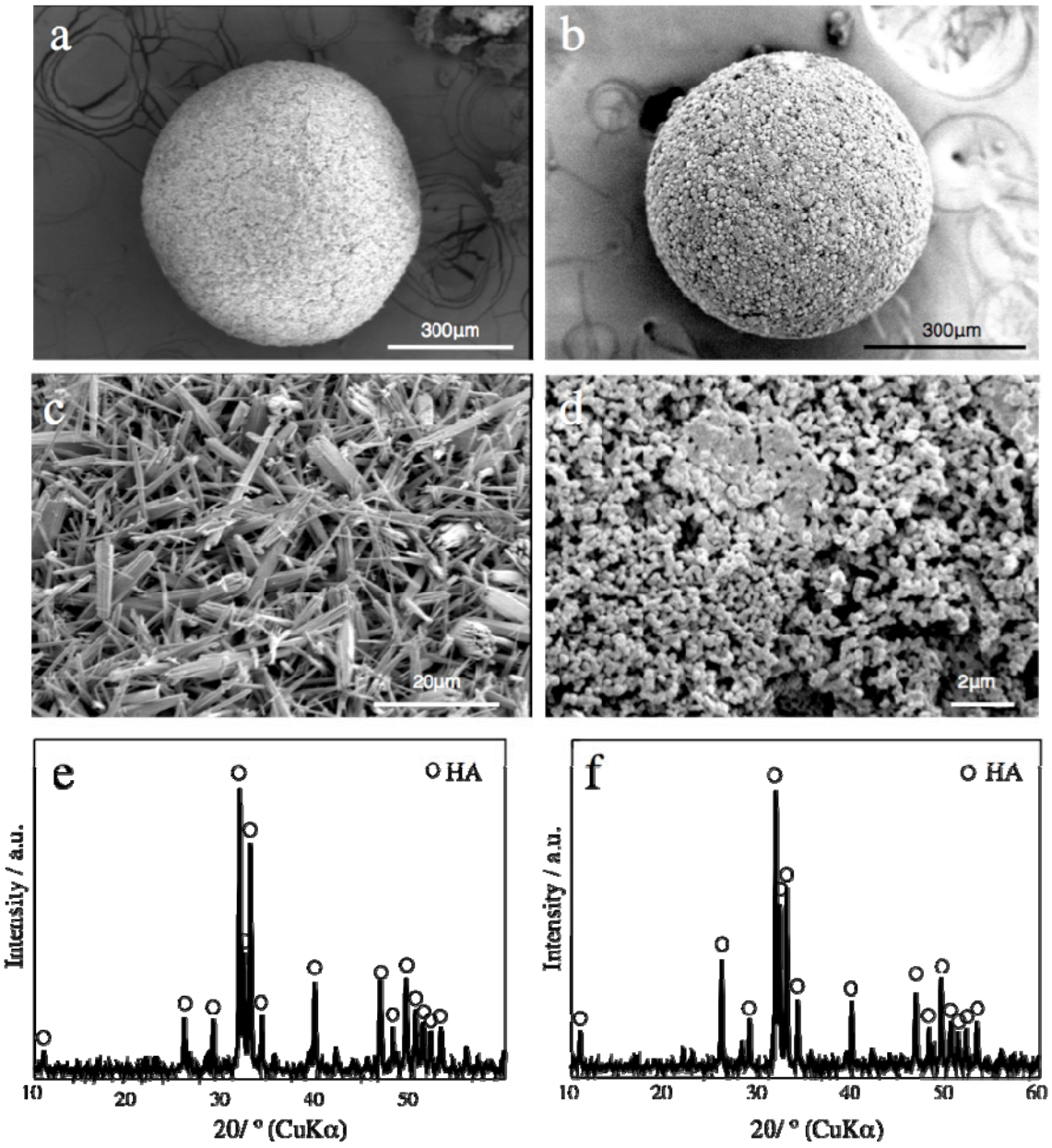
a
300μm
b
300μm
c
20μm
d
2μm
e
HA
Intensity / a.u.
10
20
30
40
50
2θ/ ° (CuKα)
f
HA
Intensity / a.u.
10
20
30
40
50
60
2θ/ ° (CuKα)

Figure 1

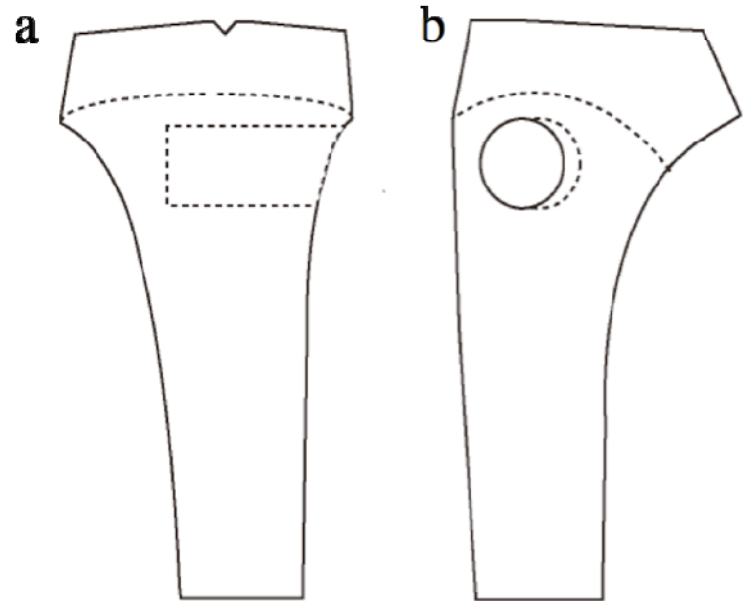

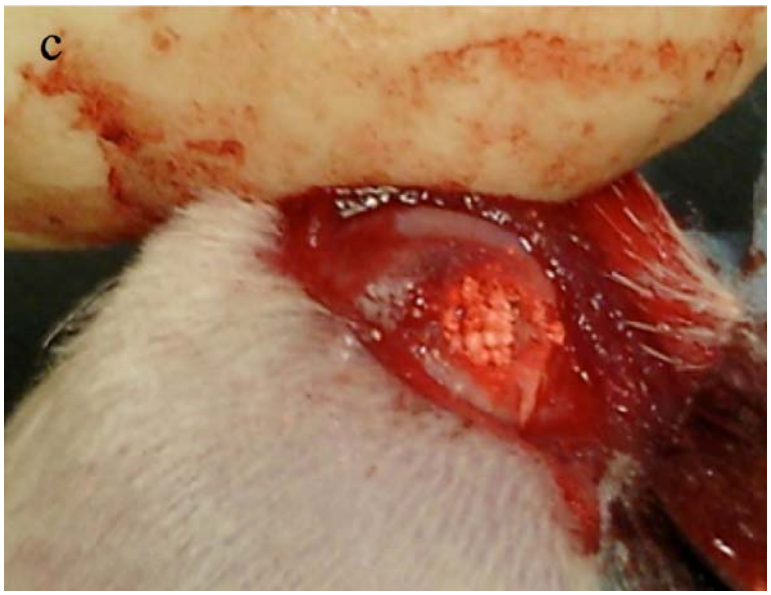

Figure 2

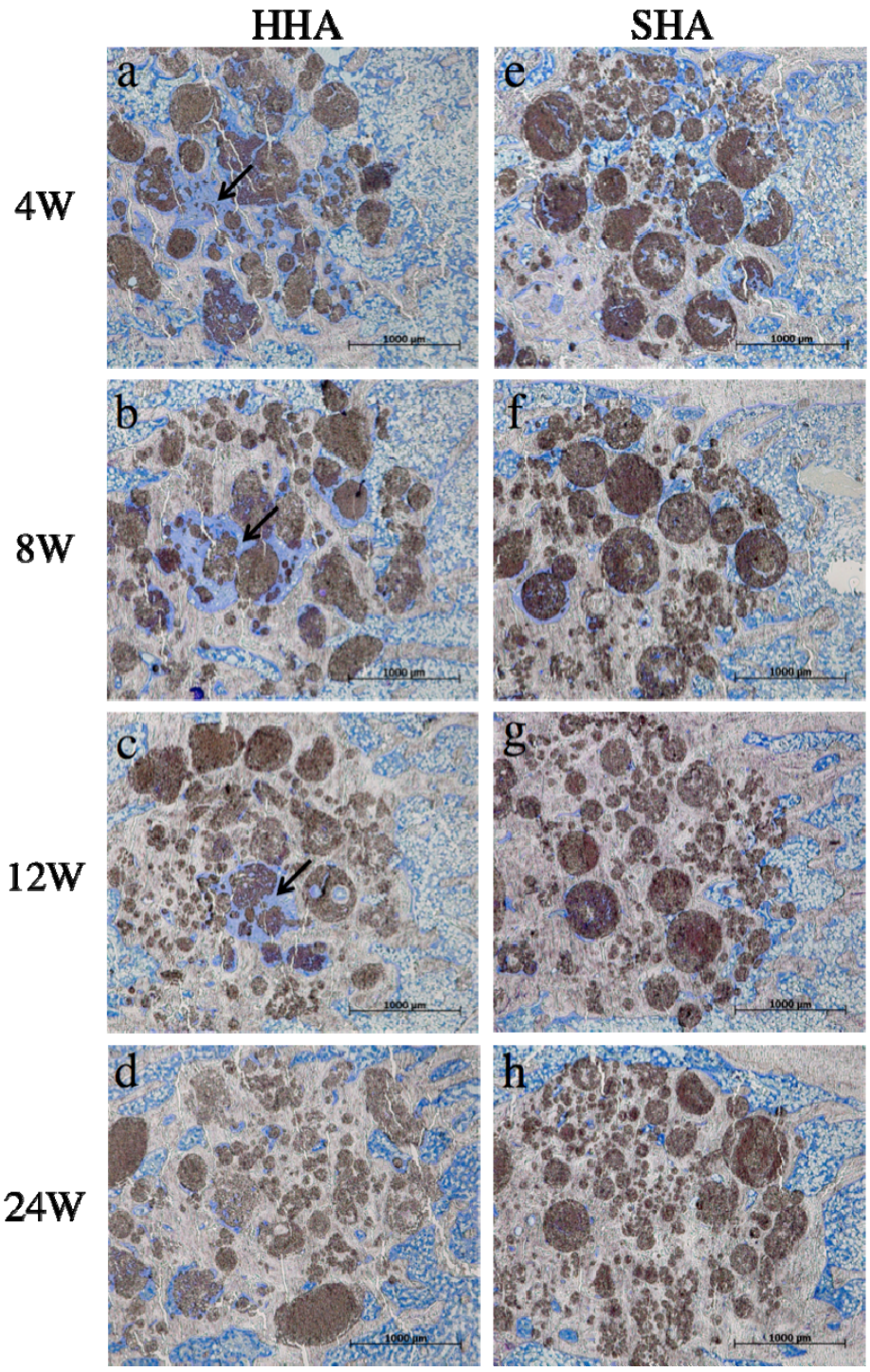

Figure 3

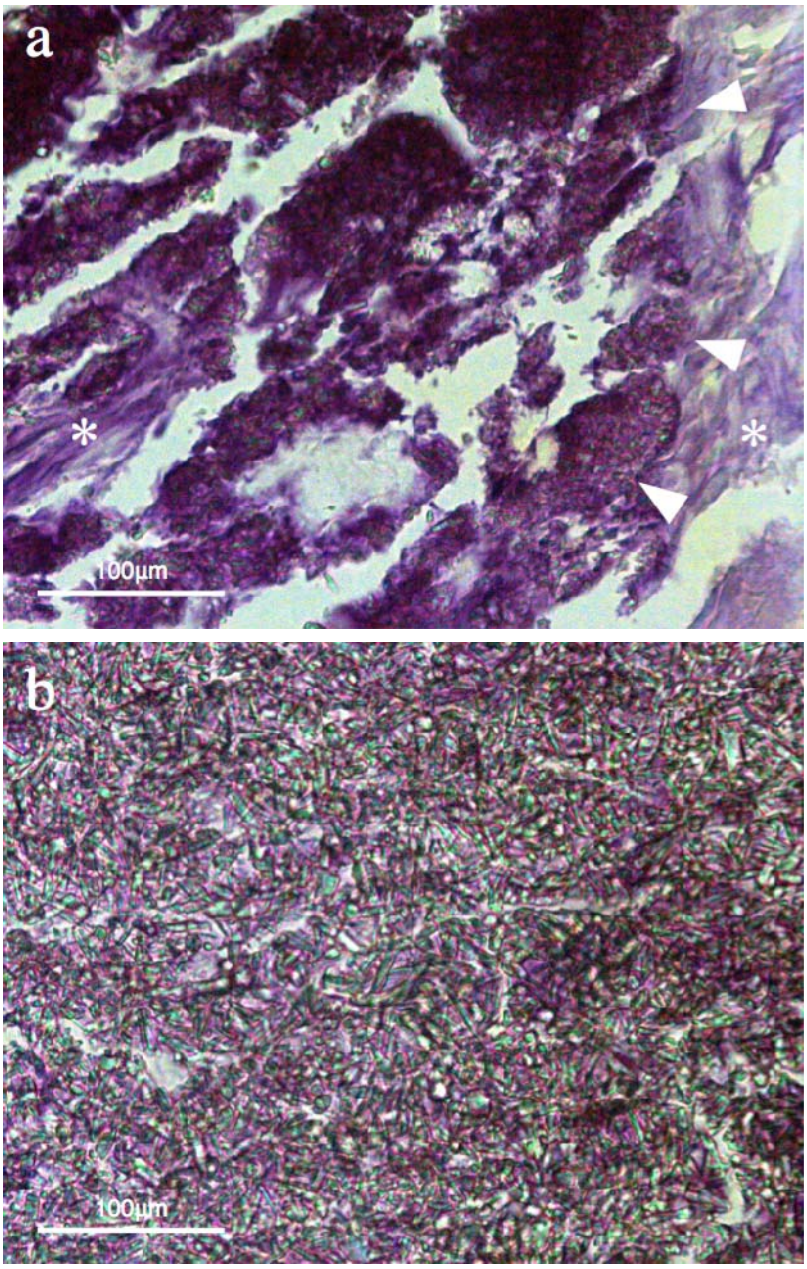

Figure 4

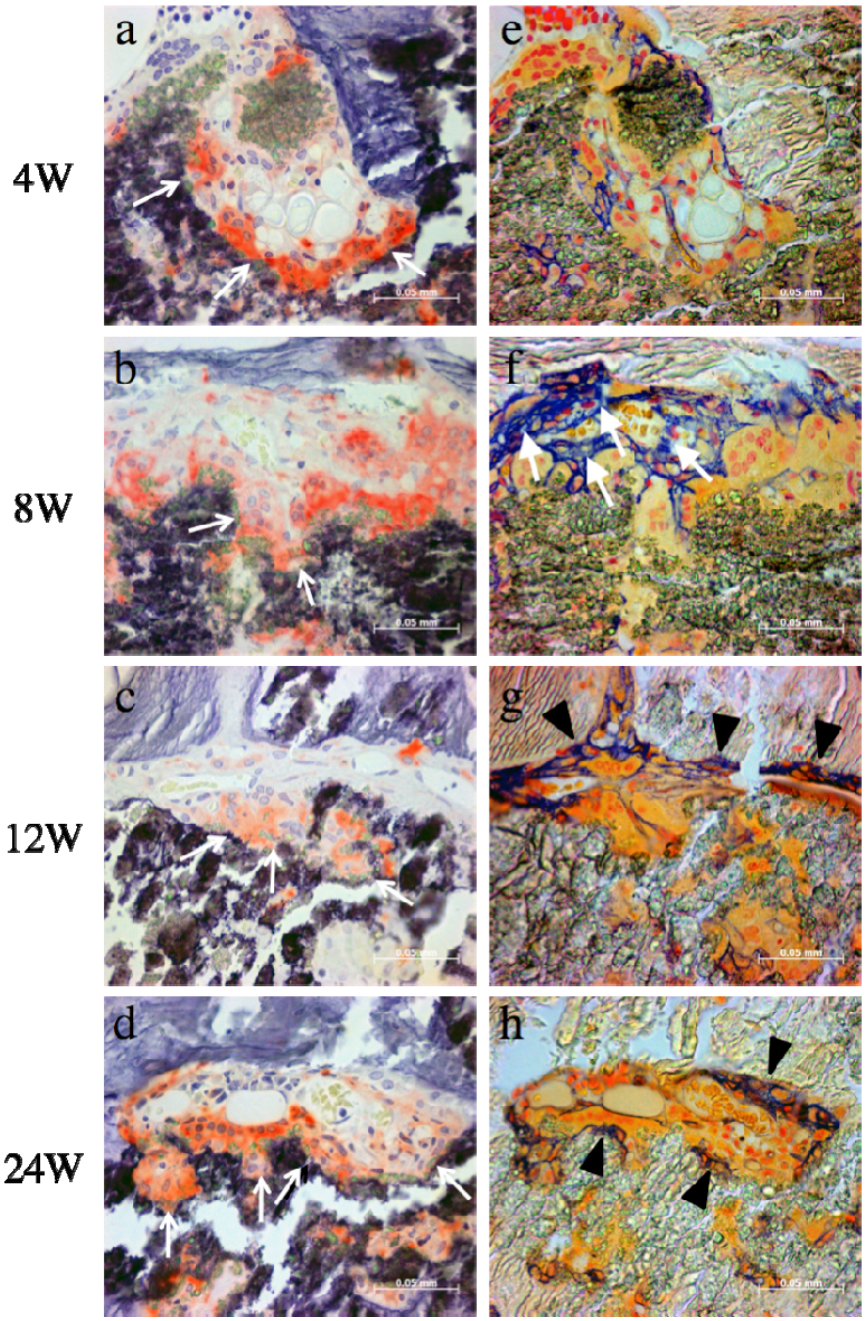

Figure 5

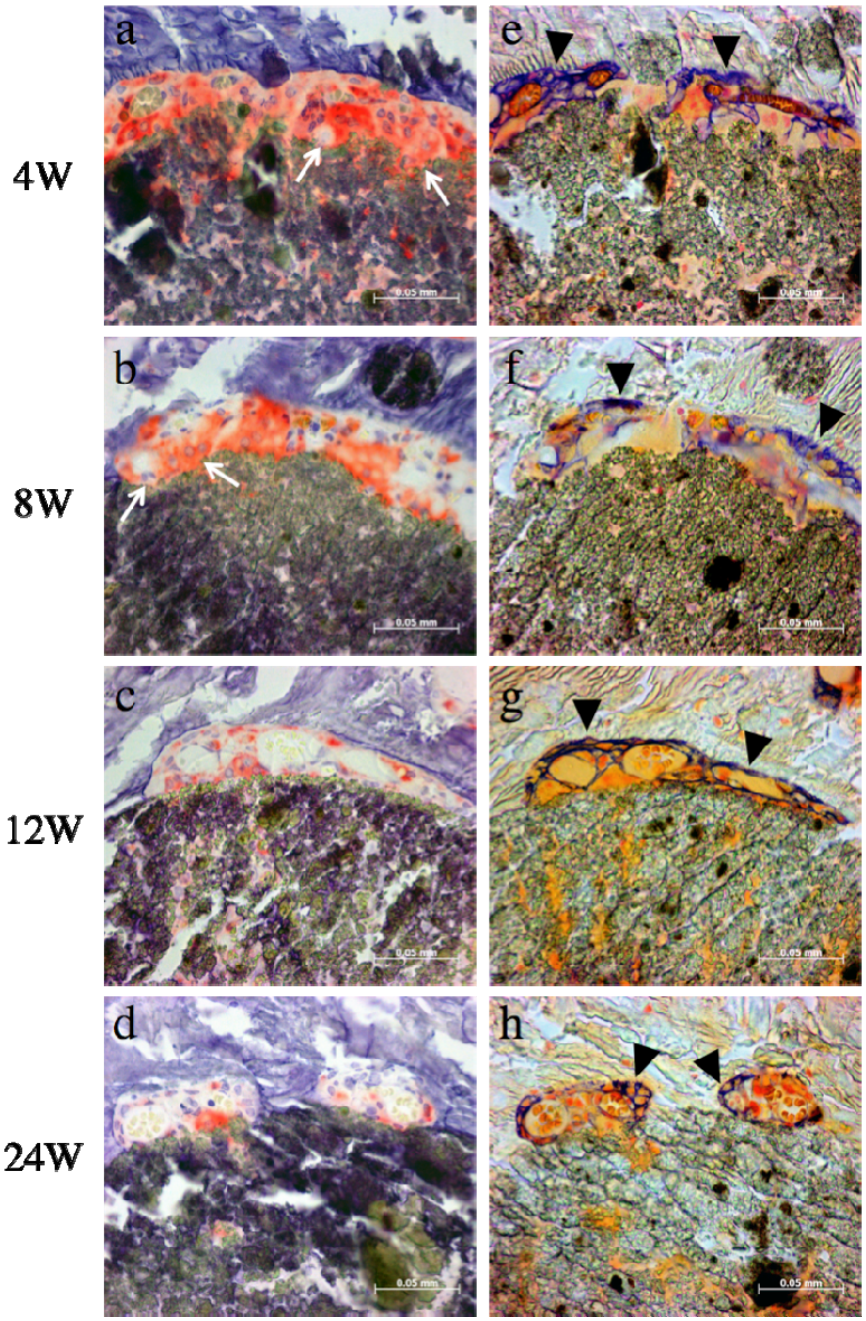

Figure 6

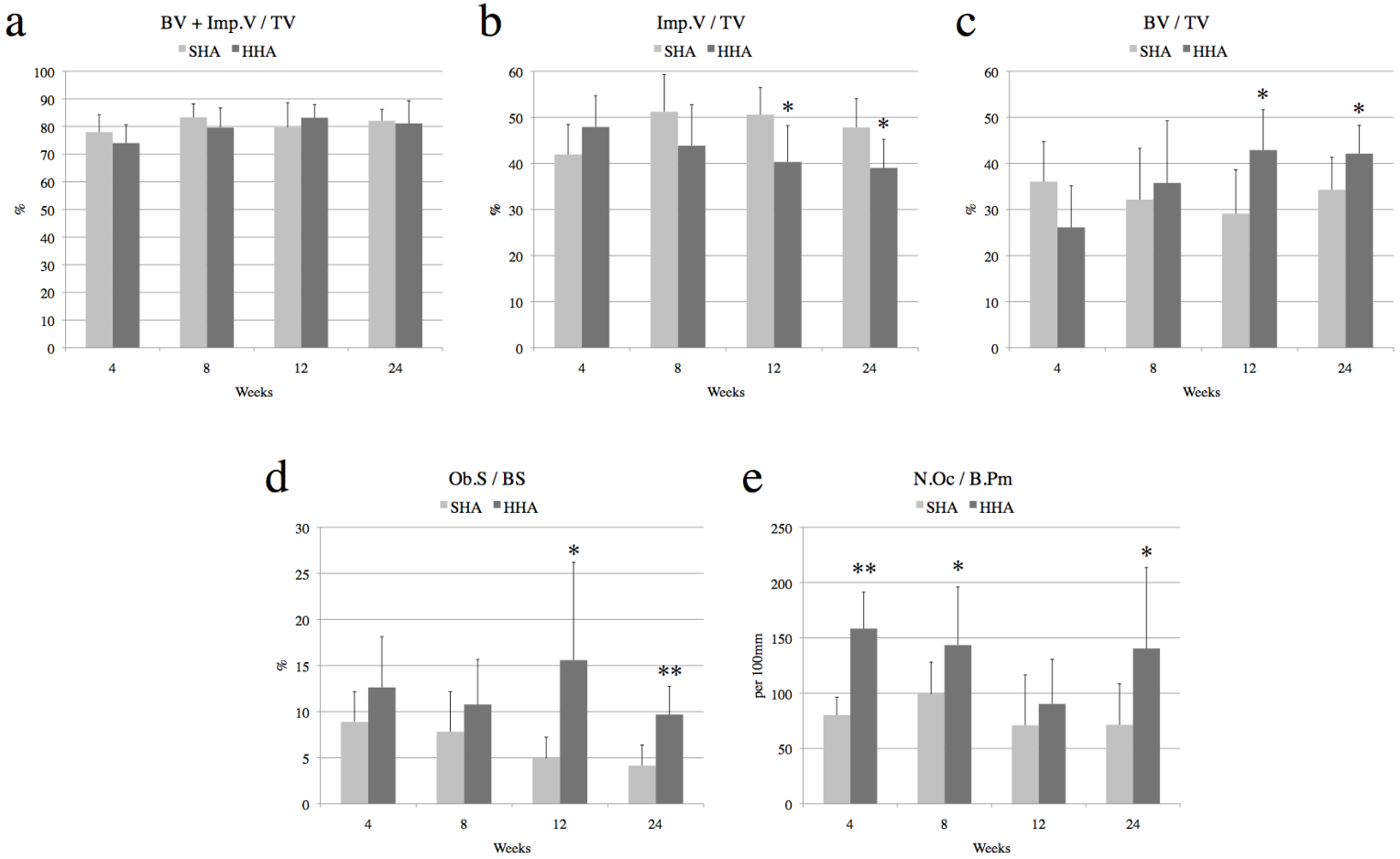
a
BV + Imp.V / TV
SHA HHA
%
Weeks
b
Imp.V / TV
SHA HHA
%
Weeks
c
BV / TV
SHA HHA
%
Weeks
d
Ob.S / BS
SHA HHA
%
Weeks
e
N.Oc / B.Pm
SHA HHA
per 100mm
Weeks

Figure 7

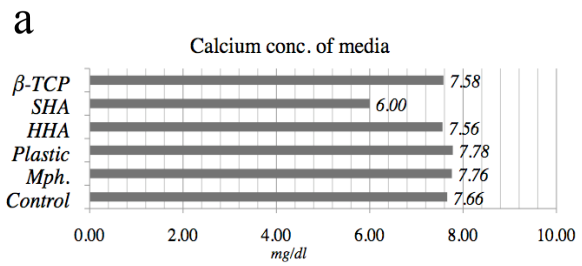

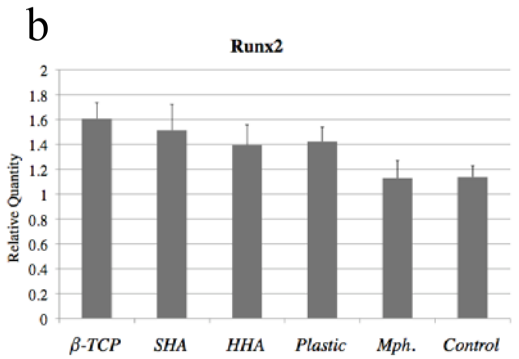

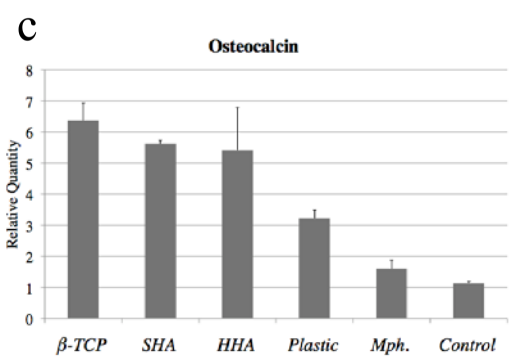

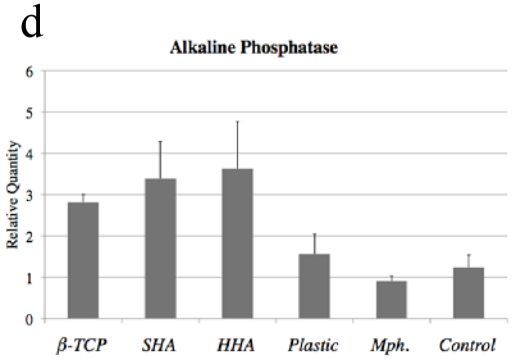

	β-TCP	SHA	HHA	Plastic	Mph.	Control
β-TCP	-				**	**
SHA		-			*	*
HHA			-		*	*
Plastic				-	*	**
Mph.	**	*	*	*	-	
Control	**	*	*	**		-

	β-TCP	SHA	HHA	Plastic	Mph.	Control
β-TCP	-			**	**	**
SHA		-		**	**	**
HHA			-		*	**
Plastic	**	**		-	**	**
Mph.	**	**	*	**	-	*
Control	**	**	**	**	*	-

	β-TCP	SHA	HHA	Plastic	Mph.	Control
β-TCP	-			**	**	**
SHA		-		*	*	**
HHA			-	*	*	**
Plastic	**	*	*	-		
Mph.	**	*	*		-	
Control	**	**	**			-

Figure 8